Microwave Non-Destructive Evaluation of Corrosion in Reinforced Concrete Structures

G. Roqueta*†, L. Jofre* and M. Feng†
*AntennaLab. Department of Signal Theory and Communications. Universitat Politècnica de Catalunya
Spain
gemma.roqueta@tsc.upc.edu
†Department of Civil and Environmental Engineering, University of California Irvine (UCI), United States

***Abstract*—This paper presents a proof of concept of a Non-Destructive microwave imaging technique for the determination of the corrosion percentage in reinforced concrete structures. This technique is based on a combination of frequency domain measurements of the scattering signature of the concrete structure and the application of thermal induction on the rebar surface. The propagation of the electric fields through the structures is simulated using the scattering theory for metallic cylinders. Transmission measurements on test samples with different cover depths and corrosion percentages of the rebars are performed showing promising results on the detection and quantification of the corrosion in reinforced structures.**

I. Introduction

Corrosion in steel reinforced concrete (RC) structures is one of the main causes of cracks and deterioration of concrete, leading to the early failure of RC structures with fatal human consequences. These consequences are not only related to severe damage to human beings (a sad example is the collapse of a concrete highway viaduct segment in Canada due to rebar corrosion in which five lives were lost [1]) but also to a global cost of corrosion in the US of $276 billion per year [2]. Consequently, a rapid and efficient detection of the corrosion could lead to cost savings of billions of dollars per year.

Although some of the electro-chemical sensors for corrosion monitoring appear to be effective, they cannot be applied to existing RC structures whose rebars are embedded in concrete. In this regard, some Nondestructive Techniques (NDT) have been studied, but they all have their limitations and drawbacks. For instance, X-rays or ultrasounds can measure changes in density and cracks with high accuracy respectively, but they have certain safety requirements or may be very sensitive to surrounding changes (vibrations, changes on temperature, humidity, etc). To overcome these difficulties, a NDT for corrosion detection based on a combination of frequency domain microwave imaging and thermal induction is proposed in this paper.

II. Principle of thermal induction in RC

The technique proposed herein consists on performing microwave thermally induced differential measurements on RC structures with corroded and non-corroded steel to assess its capability to quantify the amount of corrosion on the rebars. Given the capability of microwaves to sense and penetrate light-opaque materials with sufficient resolution and penetrability, they are aimed to provide response sensitive enough to the corrosion amount variations given a certain geometry. In addition, microwaves are believed to be able to measure changes in temperature of electrically soft materials such as concrete, since microwaves are sensitive to the temperature induced conductivity and resistivity changes. Electrical conductivity is strongly dependent on temperature following a non-linear dependence. However, the degree of nonlinearity is relatively small in a temperature range of environmental monitoring, and a linear equation [3] is commonly used to represent this relation:

$$\sigma_t = \frac{\sigma_0}{1+\alpha(T-T_0)} \tag{1}$$

where σ_0 is the electrical conductivity at the temperature T_0=20 °C, σ_T is the electrical conductivity at the measured absolute temperature T and α is the temperature coefficient of resistance [4]. This equation is represented in Fig. 1, where it can be seen that for the most common temperature variations in environmental monitoring, the steel preserves its conducting properties.

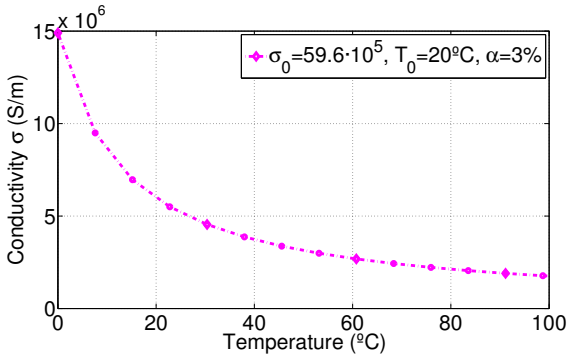

Fig. 1. Evolution of the conductivity depending on the temperature difference $(T-T_0)$.

It has been proven in [5], using both conventional thermocoupler and infrared (IR) thermography, that concrete with corroded steel and rust has a better capability to absorb and release heat, showing faster heating and cooling rates than the one with non-corroded steel rebar. Hence, the heating and cooling rates compared to those measured on a non-corroded

sample are believed to provide information about the corrosion amount on a reinforced concrete structure.

In this technique the rebar embedded in the concrete is heated by an electromagnetic high-frequency alternating current (AC) electrical inductor. The radio frequency (RF) electrode is applied to one of the concrete surfaces, the metallic rebar is remotely heated and the heat is transferred to the concrete surface. In average, the temperature at the edges of the rebar (that are exposed to air in the present RC samples) will increase 1°C every 3 minutes. Slight variations of this figure may occur depending on the cover depth (distance between the concrete surface and the closest rebar surface) of the sample. Then, the RF electrode is removed and two microwave sensors are placed in a transmission arrangement to monitor the s-parameters during a certain time period.

III. Modeling of the Geometry

The study is focused on the analysis of two specific RC samples with different concrete cover depths and a rebar diameter of $2r_0$=1.25 cm (4/8" according to the standard nomenclature for rebar diameters). Fig. 2 shows a scheme of these two samples. Samples of type A have a cover depth of c_d=3.75 cm (1.5") and a total width of d_m=8.75 cm. Samples of type B have a cover depth of c_d=5 cm (2.0") and a total width of d_m=11.25 cm.

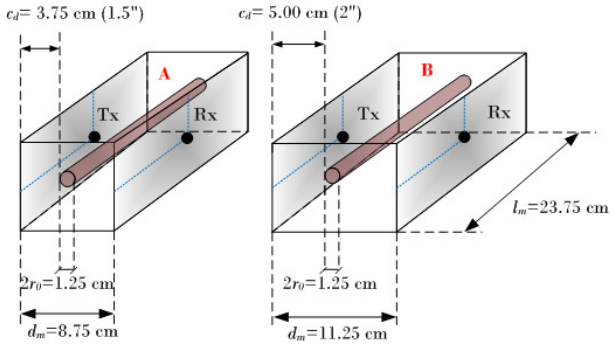

Fig. 2. Scheme of the two types of blocks used in this experiment with different cover depths. Blocks of type A have cover depth of c_d=1.5" and blocks of type B have a cover depth of c_d=2".

Three different samples of each type are fabricated with different degrees of corrosion induced on their rebars. The impressed current method [6] is used to accelerate corrosion on the rebars. Samples with 0%, 10% and 30% corrosion percentages are fabricated. The corrosion amount on a rebar is typically calculated as the percentage of weight lost with respect to a non-corroded rebar. Although the corrosion process may not be uniform along the rebar, it could be assumed that the loss of weight is equivalent to a uniform loss of volume on the rebar, thus simplifying the model of the geometry. For a N% corrosion amount the overall weight is reduced in N% and so the overall volume is. As a consequence, the final radius of the rebar can be expressed as:

$$r_{met} = \sqrt{1 - N} r_0 \tag{2}$$

where $2r_0$ is the initial diameter of the rebar. In addition, it has been reported in [7] that when the volume of the rebar is reduced due to heavy corrosion, a volume of rust appears surrounding the rebar and occupying four times the corresponding loss of volume in the rebar . Then the outer radius of the rust area can be written then as:

$$r_{oxi} = \sqrt{1 + 3N} r_0 \tag{3}$$

This data can be helpful to consider a layered scenario for simulations. The rust can be modeled as a new hollow cylinder surrounding the steel rebar. This cylinder has a certain thickness filled by a dielectric material which is the rust layer. The higher the amount of corrosion, the thicker the hollow cylinder is and the thinner the rebar is. Fig. 3 shows how the inner rebar is reduced when the amount of rust increases.

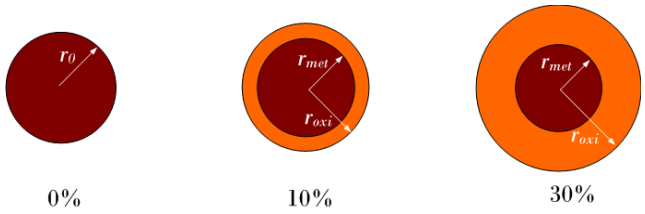

Fig. 3. Variation of the rebar and rust diameters for different corrosion percentages.

IV. Scattering Principle of a PEC Cylinder

Being the steel rebar considered as a scattering cylinder embedded inside a layered dielectric medium, an analytical study of the variations of the total received field depending on the geometry and composition is performed based on the formulation for scattering cylinders and cylindrical wave incidence [8]. This formulation considers the simplified model of a Perfect Electric Conductor (PEC) cylinder with radius r_{met} embedded in a lossless medium with an equivalent effective permittivity that depends on the corrosion amount. That is, the equivalent effective permittivity is considered to be higher for higher corrosion. The transmitting and receiving current filaments are placed parallel to the cylinder at a distance ρ' and ρ from the cylinder center respectively, as shown in Fig. 4.

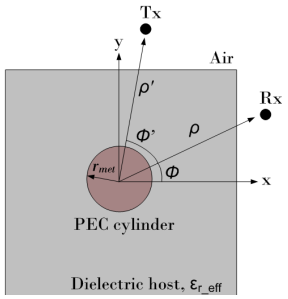

Fig. 4. PEC cylinder embedded in a dielectric host medium with effective permittivity ϵ_{r_eff}.

According to this formulation the total received field may be expressed as:

$$E_z^d = E_z^i + E_z^s = \frac{-k^2 I}{4\omega\epsilon_{r\_eff}\epsilon_0} \sum_{n=-\infty}^{\infty} H_n^2(k\rho') \begin{cases} [J_n(k\rho) - \frac{J_n(ka)}{H_n^2(ka)} H_n^2(k\rho)] e^{j\pi(\phi-\phi')} & \rho < \rho' \\ [J_n(k\rho') - \frac{J_n(ka)}{H_n^2(ka)} H_n^2(k\rho')] e^{j\pi(\phi-\phi')} & \rho > \rho' \end{cases} \quad (4)$$

Fig. 5 shows the evolution of the phase of the total received field for changes in the corrosion rate in scenarios A and B. The transmitters and receivers are located at the centers of two opposite concrete surfaces, as indicated in Fig. 2. The equivalent effective permittivity of the host medium is considered to be ϵ_{r_eff} =15 and ϵ_{r_eff} =17 in cases A and B respectively.

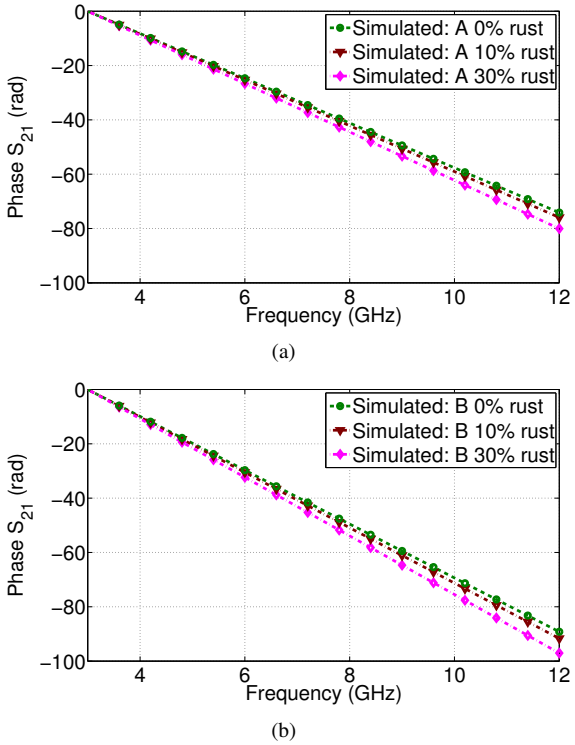

Fig. 5. Simulated variation of the phase of the total received field (S_{12}) in scenarios A (a) and B (b).

Notice that the presence of rust represents an increase of attenuation and propagation delay of the received signal in all cases. The increase of the propagation delay in the corroded rebar may be explained as a duel of consequences: on one side the reduction of the rebar diameter implies a reduction of the electrical distance for the creeping waves to propagate. On the other side, the presence of a high dielectric material surrounding the rebar makes this electrical distance longer, which leads to a strong reduction of the propagation speed. As a result of this balance, the final propagation speed with respect to the non-corroded rebar is lower, and so the propagation delay increases. Notice as well that the slope of the phase is higher in case B, since the concrete sample is thicker.

V. Measurements of the Scattering Signature of a Corroded Rebar Embedded in Concrete

Once the scattering principle of the rebar is analytically studied, preliminary frequency domain measurements using two ridge antennas (3-12GHz) in a transmission arrangement are conducted to validate the model.

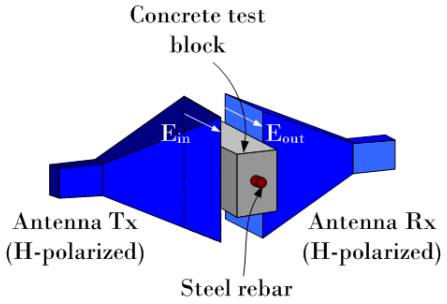

Fig. 6. Schematics of the antenna arrangement and the rebar orientation.

The relative arrangement between the antennas and the rebar is shown in Fig. 6, where the antennas and the rebar have the same polarization. Measured module and phase results of the S_{21} parameter are shown in Fig. 7 and Fig. 8. The module shows that the attenuation is higher for higher corrosion amounts. Additionally, as it was observed in the simulations of the phase in Fig. 5, the propagation velocity is lower for higher corrosion amounts. Also, differences between phase slopes are higher in case B where the distance between the rebar and the surface is higher. However, in this case the attenuation is so high that signal levels are too low (close to noise level), specially at high frequencies.

VI. Measurements of the Scattering Signature Gradient During Cooling Process

Once the main trends of the received signal depending on the cover depth and rust percentage are studied, inductive heating is applied to the concrete surface for 3 minutes. The total received signal is monitored during the first 3 hours of the cooling down process. Normalized results of the module of the received signal time-gradient in the samples of type A and B are shown in Fig. 9 and Fig. 10 respectively.

Notice that in both in Fig. 9 (b-c) and Fig. 10 (b-c), the signal gradient fades faster than in Fig. 9 (a) and Fig. 10 (a). The signal becomes stable when the temperature stabilizes as well. This means that the corroded rebar (b-c) has a faster cooling rate than the non-corroded one (a). Also, it can be observed that the gradient is less homogeneous in frequency in presence of corrosion.

VII. Conclusions

The microwave NDT presented in this paper shows promising preliminary results on the characterization of corrosion rust in RC structures. Measurements of the scattering signature

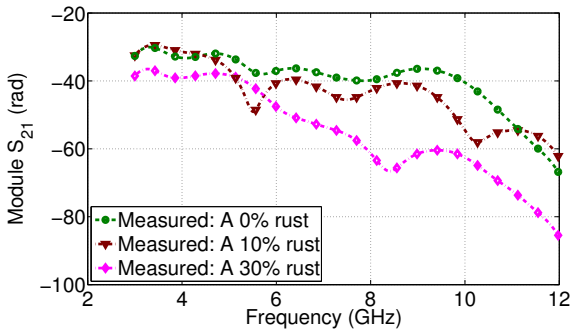

(a)

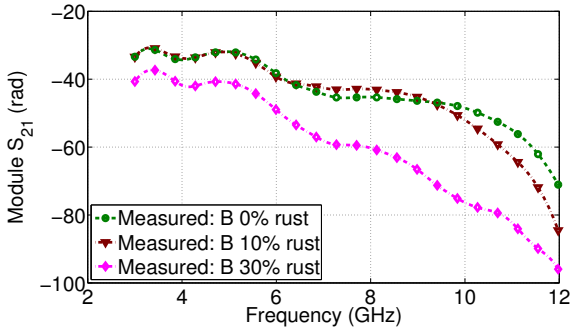

(b)

Fig. 7. Measured variation of the module of the total received field (S_{12}) in scenarios A (a) and B (b).

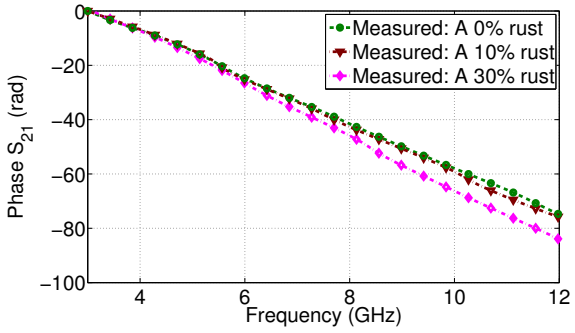

(a)

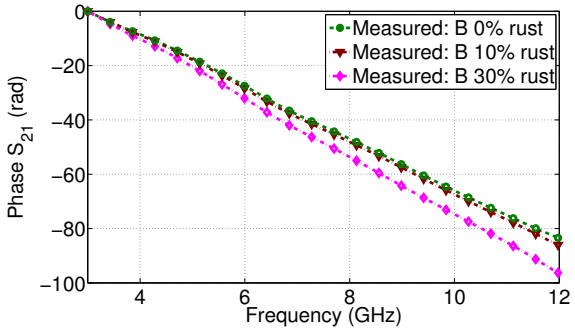

(b)

Fig. 8. Measured variation of the phase of the total received field (S_{12}) in scenarios A (a) and B (b).

of RC samples with different corrosion rate show different characteristics in relative module and phase of the received signals. Additionally, measurements during the cooling rate of the RC samples after inductive heating show different module gradients. The corroded rebars present faster cooling rate and less homogeneous gradient than the non-corroded ones. In summary, this analytical experimental study constitutes a good proof of concept for the development of a nondestructive evaluation method to detect and quantify the rebar corrosion of reinforced concrete structures, which is needed to ensure their structural safety.

ACKNOWLEDGMENTS

This work was supported in part by the Spanish Interministerial Commission on Science and Technology (CICYT) under projects TEC2007-66698-C04-01, TEC2010-20841-C04-02 and CONSOLIDER CSD2008-68 and by the "Ministerio de Educación y Ciencia" through the FPU fellowship program. The work was also supported by the Technology Innovation Program (TIP) of the US National Institute of Standards and Technology (NIST).

REFERENCES

[1] I. Rappoport, "Corroded steel reinforcing bars likely culprit," *Daily Commercial News and Construction Record*, 2006.
[2] [Online]. Available: www.corrosioncost.com
[3] P. A. Tipler and G. Mosca, *Physics for Scientists and Engineers*. Vol. 2, 5th edition, New York, 2004.
[4] D. C. Giancoli, *Physics*. 4th Ed, Prentice Hall, 1995.
[5] M. Feng, "Microwave thermoreflectance imager for corrosion detection and monitoring in reinforced concrete," Annual Report to TIP, NIST, Tech. Rep., 2010.
[6] A. C. Gangadharan, *Leak prevention and corrective action technology for underground storage tanks*, ser. Pollution Technology Review, ndc, Ed. Noyes Data Corporation, 1998, no. 153.
[7] NRMCA, "Concrete in practice: What, why and how? cip 25 - corrosion of steel in concrete," National Ready Mixed Concrete Association (www.nrmca.org), Tech. Rep., 1995.
[8] R. F. Harrington, *Time-Harmonic Electormagnetic Fields*, I. P. E. Board, Ed. The IEEE Press Series on Electromagnetic Wave Theory, 2001.

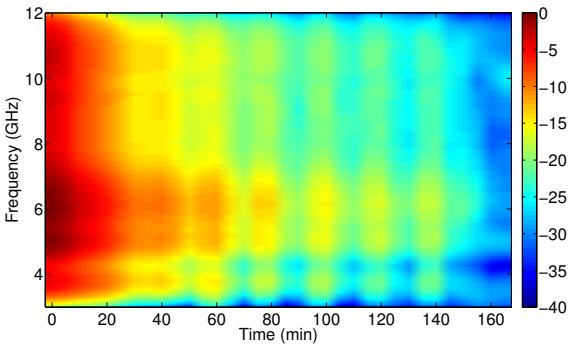

(a)

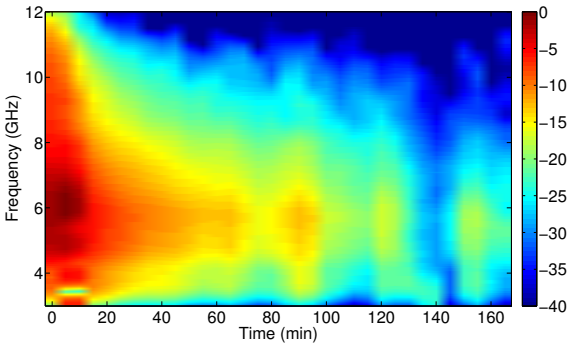

(b)

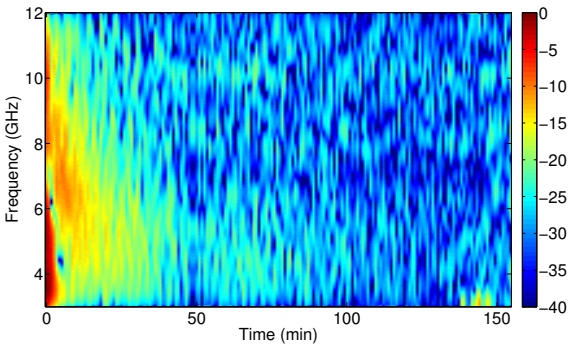

(c)

Fig. 9. Module gradient of the received signal in measurements of the reinforced concrete blocks of type A with 0% (a), 10% (b) and 30% (c) corrosion.

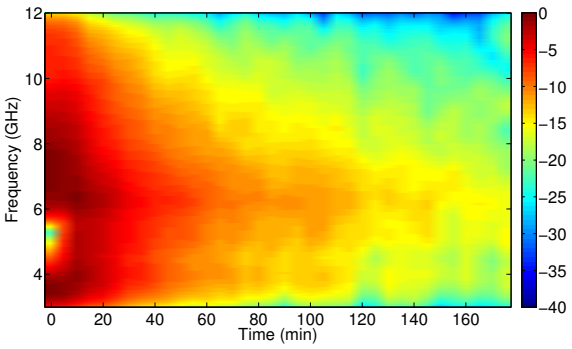

(a)

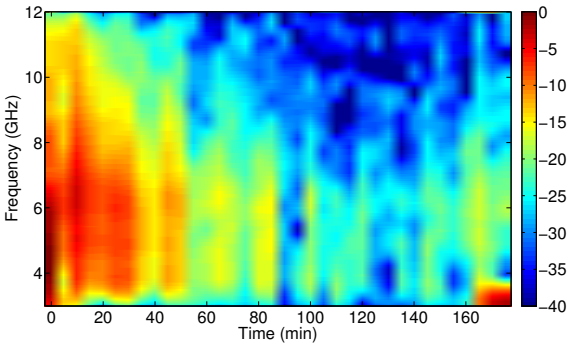

(b)

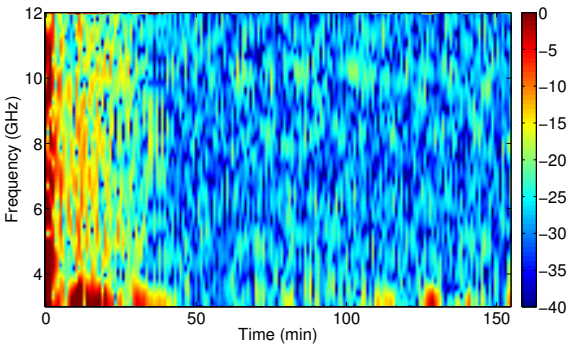

(c)

Fig. 10. Module gradient of the received signal in measurements of the reinforced concrete blocks of type B with 0% (a), 10% (b) and 30% (c) corrosion.